Composite Structures 161 (2017) 51–64

Contents lists available at ScienceDirect

Composite Structures

journal homepage: www.elsevier.com/locate/compstruct

Modeling PVC-coated polyester as a hypoelastic non-linear orthotropic material

Charles F. Jekel [a,b,*], Gerhard Venter [a], Martin P. Venter [a]

[a] Department of Mechanical and Mectronic Engineering, Stellenbosch University, Private Bag X1, Matieland 7602, South Africa
[b] Department of Mechanical and Aerospace Engineering, University of Florida, Gainesville, FL 32611, USA

ARTICLE INFO

Article history:
Received 12 October 2016
Accepted 5 November 2016
Available online 10 November 2016

Keyword:
Non-linear orthotropic, Inverse analysis
Non-linear material model
Hypoelastic material

ABSTRACT

A hypoelastic non-linear orthotropic material model was characterized for two different PVC-coated polyesters from uniaxial tests in the warp, fill, and 45° bias yarn directions. Ultimately the non-linear orthotropic material model fails to capture the full behavior of PVC-coated polyester. Thus the determination of material parameters depends upon which experimental response is the most important for the model to capture. Two methods are presented for determining different parameters for the non-linear orthotropic material, such that each method captures a particular aspect of the material's response better than the other method. The first approach derives the stiffness moduli as a function of strain from the experimental stress–strain response of the uniaxial tests. The second approach utilizes an inverse analysis, powered by an optimization routine, to find the best material parameters such that the experimental load–displacement response is matched in the finite element (FE) model. Additional the Poisson's effect was investigated, and the transverse uniaxial behavior is presented.

1. Introduction

Coated fabrics, such as PVC-coated polyester, or other technical woven textiles are used in membrane structures. The design of membrane structures often requires some form of numerical analysis. PVC-coated polyester is generally modeled as a plane stress linear orthotropic thin shell in finite element (FE) analyses [1–4], because modeling the fiber interactions for a complete structure is too computationally expensive [5]. The linear orthtropic material models have been widely used despite PVC-coated polyester fundamentally violating the plane-stress assumption used by conventional FE analyses [6]. A non-linear material model may more accurately represent the complex behavior of PVC-coated polyester. For this reason, a hypoelastic plane stress non-linear orthotropic material model was selected for modeling PVC-coated polyester and other complex composite materials.

PVC-coated polyester exhibits anisotropic behavior, however the material is often simplified to behave as an orthotropic material [7]. The load–displacement response of PVC-coated polyester is highly non-linear [8]. Galliot and Luchsinger [9] defined a non-linear material model for PVC-coated polyester that was load-ratio dependent, and determined from biaxial tests of varying load-ratios. Ambroziak and Kłosowski [10] took a different approach, and defined a tri-linear orthotropic material model. The tri-linear model picked different stiffness moduli based on the elemental strain values. Both of these material models offer improvements over the traditional linear-elastic plane-stress orthotropic material model for PVC-coated polyester, but are limited to only capturing some representative response of the non-linear behavior.

A material model that may be an improvement from the previous work exists in the NLELAST model definition of MSC Marc [11]. The NLELAST model includes a simplified non-linear elastic orthotropic material model, which may be suitable for modeling PVC-coated polyester. The material model is a plane stress hypoelastic orthotropic material model for thin shell elements, where the Young's moduli (E_1, E_2), Poisson's ratio (ν_{12}), and shear modulus (G_{12}) can be defined as functions of the strain component in their respective directions. This hypoelastic non-linear orthotropic material model for PVC-coated polyester may be useful in the design and analysis of structures that may operate in the non-linear region, while potentially providing an improved representation of the complex load–displacement behavior of the material.

With a material model chosen, the next step is to determine the appropriate material model parameters. Inverse analyses can be a useful way to characterize material parameters for the FE method.

* Corresponding author at: Department of Mechanical and Aerospace Engineering, University of Florida, Gainesville, FL 32611, USA.
E-mail address: cjekel@gmail.com (C.F. Jekel).

http://dx.doi.org/10.1016/j.compstruct.2016.11.019
0263-8223/

In this context, an inverse analysis is the process of using numerical optimization techniques to determine the material parameters such that a FE model matches the behavior of a physical test. One benefit of an inverse analysis is that the material may be characterized with a load state that is more complex than traditional uniaxial or biaxial testing. Garbowski et al. [12] set up an inverse analysis to characterize paper samples with an orthotropic elastic–plastic hardening model. A hole was cut in the center of the biaxial samples to increase the inhomogeneous response of the specimens. Modeling materials from a complex state may provide more insight when modeling various composite structures.

In this investigation two PVC-coated polyesters are considered. The first is the VALMEX® 7318 5340, and the second is Cape Coaters (Pty) Ltd CF0700T. Two characterization methods are proposed to determine a non-linear orthotropic material model. The direct method assumes a stress–strain conventional continuum model, while the inverse method matches the materials load–displacement behavior. At the start of the project it was unknown which method will produce a non-linear orthotropic material model that more accurately represents the behavior of PVC-coated polyester. PVC-coated polyester violates the plane stress and continuum assumptions. It was a concern that simply matching the in plane stress–strain behavior is no guarantee that the load–displacement behavior will also be matched, and vice versa because of violations in the plane stress and continuum assumptions.

The purpose of this paper is to provide two methods for characterizing a material with the non-linear orthotropic material model. All the parameters used for a non-linear orthotropic material model on two different types of PVC-coated polyesters are presented in this paper. A direct method and an inverse method were used to determine the material parameters. Poisson's behavior of the material is investigated, and the limitations of the non-linear orthotropic material model are discussed.

2. Uniaxial tests

The properties of the two types of PVC-coated polyester tested are listed in Table 1. All of the properties provided, with the exception of the material thickness, come directly from the manufacturer. The thickness was obtained from the average of ten measurements taken on the uniaxial samples.

Uniaxial tests were conducted for both PVC-coated polyesters in the material warp, fill, and 45° bias yarn directions. For each material yarn direction, five uniaxial tests were performed. The tests were performed following the ASTM D751 standard [13] cut strip test method on a MTS Criterion® 44. Test specimens were prepared to be 25 mm in width and 175 mm in length. Clamps 30 mm wide were used to hold the specimens sufficiently flat and parallel during the test. The distance between the clamps at the start of the test was 75 mm as prescribed by the ASTM D751 standard.

Utilizing Digital Image Correlation (DIC) [14,15], a virtual strain gauge was used to track the displacement of the specimens. This virtual strain gauge data was the only data considered in the characterization of the non-linear orthotropic material parameters. Finite element (FE) models were constructed to replicate the physical conditions of the uniaxial test. The results of the FE models with the non-linear orthotropic material models were compared to the physical behavior of the virtual strain gauges to demonstrate the effectiveness of the material models.

The DIC generates points on the surface of an uniaxial specimen in three dimensions. Virtual strain gauges track the displacement between two points on the surface of the uniaxial specimens. A single virtual strain gauge was placed approximately in the center of each uniaxial test. The length of the various strain gauges used can be seen in Table 2. The strain gauge lengths were chosen to match points in the calculated full displacement field as best as possible, attempting to avoid interpolation error. The difference in initial strain gauge lengths resulted from subtle differences in the parameters used to calculate the displacement field.

Table 1
Properties of the tested PVC-coated polyester.

	VALMEX® 7318	CF0700T
Warp tensile strength (ISO 1421 N/50 mm)	3000	1600
Fill tensile strength (ISO 1421 N/50 mm)	3000	1350
Grams per square meter (g/m^2)	1000	700
Thickness (mm)	0.81	0.55

Table 2
Initial virtual strain gauge length l_i for material test direction.

Direction	l_i (mm)
Warp	20.0
Fill	22.8
45° Bias	19.8

Three non-linear FE models were created in MSC Marc to replicate the three distinct uniaxial tests in the warp, fill, and 45° bias material directions respectively. Symmetry is utilized to simplify the uniaxial FE models in the warp and fill directions. However, the 45° bias FE model could not take advantage of reflective symmetry as the test produced an unsymmetrical displacement field. The FE models of the warp and fill direction only model the area of the virtual strain gauge, while the entire sample is modeled between the grips for the 45° bias FE model because of the unsymmetrical response. The mesh used for the warp uniaxial test is seen in Fig. 1, while a similar mesh is used in the fill direction. The virtual strain gauge location on the 45° bias mesh can be seen by the two green dots in the center of Fig. 2.

The Young's moduli (E_1, E_2), Poisson's ratio (ν_{12}), and shear modulus (G_{12}) are defined as functions of the strain component

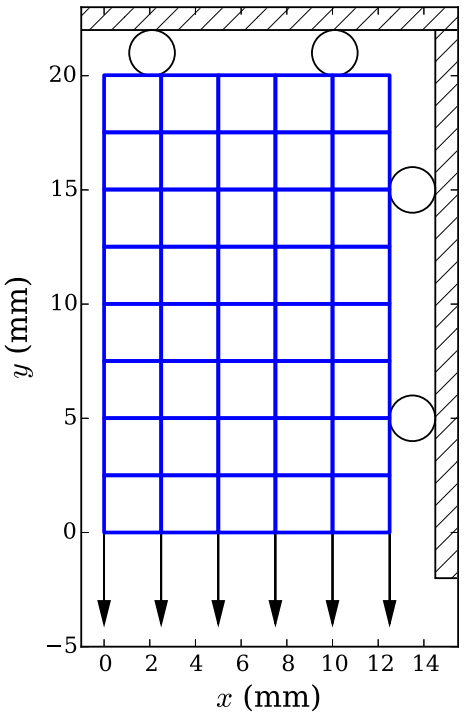

Fig. 1. Symmetric FE mesh of the warp uniaxial test with boundary conditions.

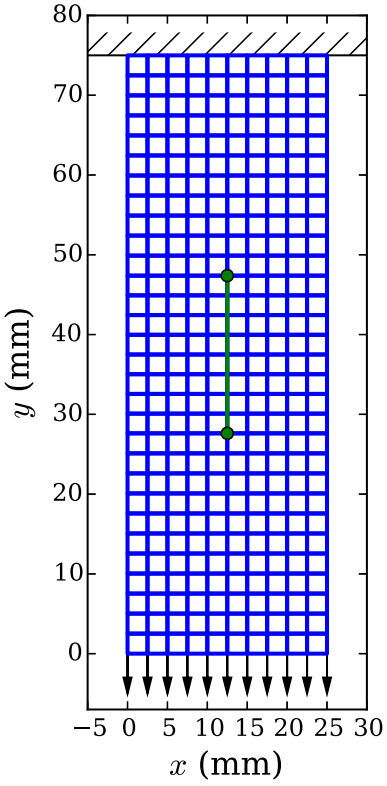

Fig. 2. 45° bias uniaxial test FE mesh with boundary conditions and virtual strain gauge indicated by the green dots in the center of the mesh.

in their respective direction for the non-linear orthtropic material model. MSC Marc allows for the material model to define Poisson's ratio as a function of strain. However having Poisson's ratio as a function of strain presented a computational concern for the inverse problem, specifically how to determine this function. Thus it was assumed that Poisson's ratio was to be a fixed constant. The next section explains how the Poisson's ratio was determined.

3. Poison's ratio

The Poisson's ratio (ν_{12}) can be expressed as the ratio of the negative transverse strain to the axial strain for a uniaxial test in the warp direction. It is possible to add an additional virtual strain gauge in the transverse direction to approximate the Poisson's ratio of the PVC-coated polyester from the uniaxial tests. A transverse strain gauge was added to every uniaxial test, with a length of 15.0 mm. The length was chosen to avoid edge effects, while still being large enough to capture the transverse response. Only ν_{12} is needed to define the Poisson's ratio for a constant thickness orthotropic material model, as ν_{21} is determined through the material model. We can use the test results from the uniaxial warp direction to approximate Poisson's ratio, because we have set up the material warp direction to align with the primary direction in our material model.

The Poisson's ratio was calculated for the VALMEX® 7318 and CF0700T at various loads of the warp uniaxial tests. The results are presented in Figs. 3 and 4. It can be noted that the Poisson's ratio varies as the load of the material changes. There is extremely large variation between tests in the determined Poisson's ratios. A rudimentary approach was taken to deal with this variation, by simply taking the average Poisson's ratio ν_{12} from the warp tests. It was then assumed that this average Poisson's ratio was a constant in the numerical models. The average Poisson's ratio of the VALMEX® 7318 was found to be 0.136, while 0.072 was the average Poisson's ratio for CF0700T. The transverse displacements from the uniaxial tests and FE models are presented in the results section of this paper.

It is important to consider the effects of the Poisson's ratio on the FE models before characterizing the non-linear orthotropic material models. A sensitivity study was performed on the axial loads and traverse displacements of the numerical models in the warp, fill, and 45° bias material directions. The sensitivity of the axial load to Poisson's ratio is seen in Fig. 5. It is noted that the warp and fill uniaxial models are hardly affected by changes in ν_{12}, while the 45° bias uniaxial test is strongly linked to the value of ν_{12}. The sensitivity of the transverse displacement to Poisson's ratio is presented in Fig. 6. As expected the transverse displacement of the material warp and fill uniaxial tests are dependent

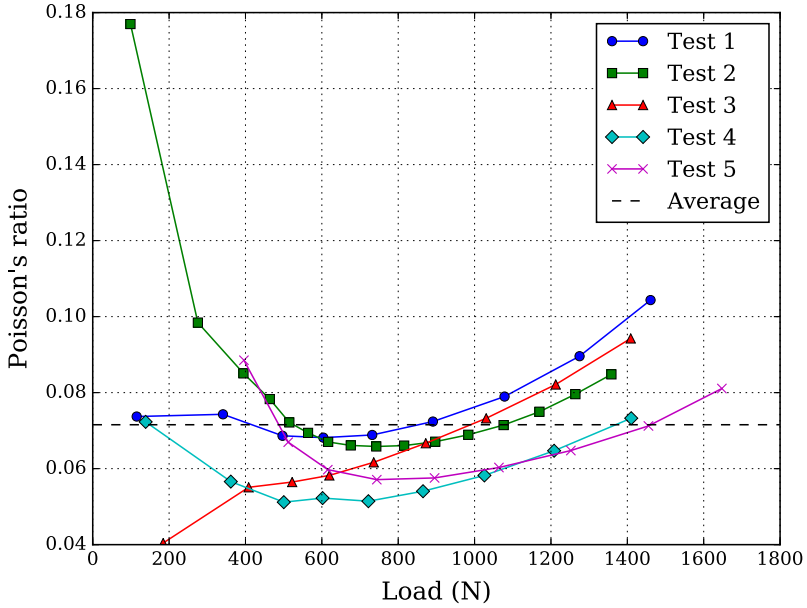

Fig. 3. Poisson's ratio (ν_{12}) for various loads from the warp uniaxial test on VALMEX® 7318.

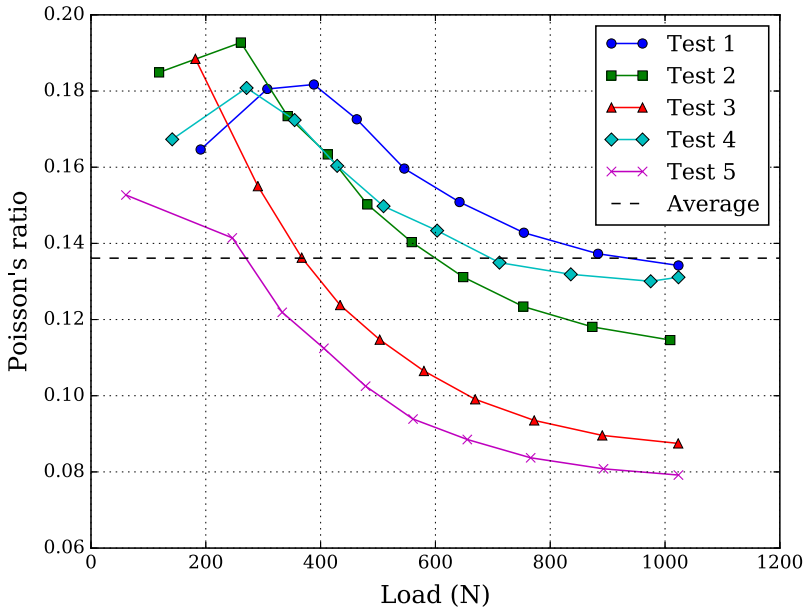

Fig. 4. Poisson's ratio (ν_{12}) for various loads from the warp uniaxial test on CF0700T.

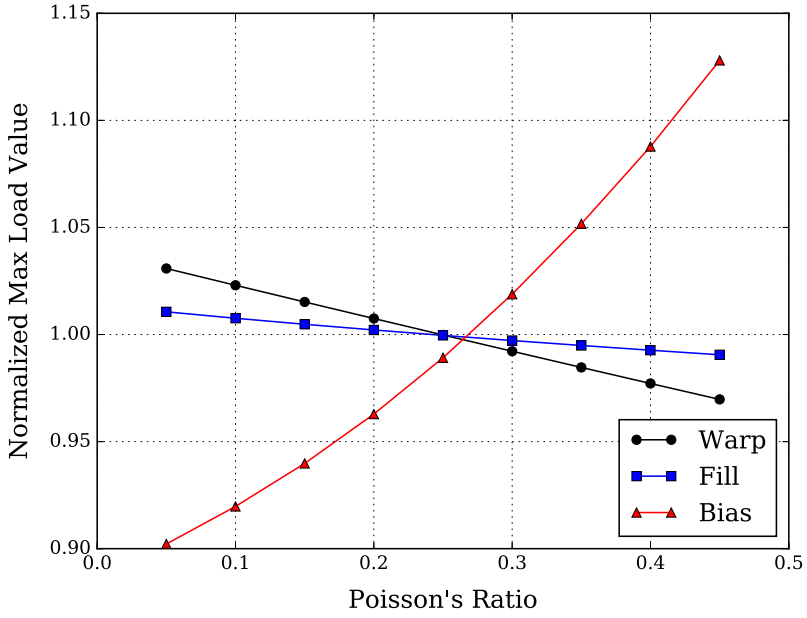

Fig. 5. The sensitivity to Poisson's ratio of the axial load in the FE models of the warp, fill, and 45° bias uniaxial tests.

on ν_{12}. The 45° bias uniaxial test appears to have similar sensitivity to the Poisson's ratio in both the transverse and axial directions. With the sensitivity study it was concluded that the 45° bias FE model was dependent on both ν_{12} and G_{12}, as both variables strongly influence the 45° bias response. There is a likelihood that this dependency may result in different combinations of ν_{12} and G_{12} producing similar behavior. Thus the simultaneous optimization of ν_{12} and G_{12}, with the 45° bias FE model, may result in a non-unique solution.

4. Characterization method 1: direct stress–strain approach

The first method for characterizing the non-linear orthotropic material model uses stress and strain to determine stiffness moduli as a function of strain. The engineering strain values were calculated from the virtual strain gauges on all of the uniaxial tests. The engineering stress values were calculated by dividing the total load by the initial cross sectional area of the test specimens. Engineering stress and strain are used as opposed to true stress and strain, because the non-linear orthotropic material model does not account for through thickness change of the material. Thus the FE model is not capable of determining either true stress or true strain. In addition, the thickness change of the materials during the uniaxial tests were not measured.

The stress–strain data from the uniaxial tests on the two materials is presented in Figs. 9 and 10. Data points in the figures are from all five uniaxial tests. A polynomial was fitted to the stress–strain data for each material direction using the least squares

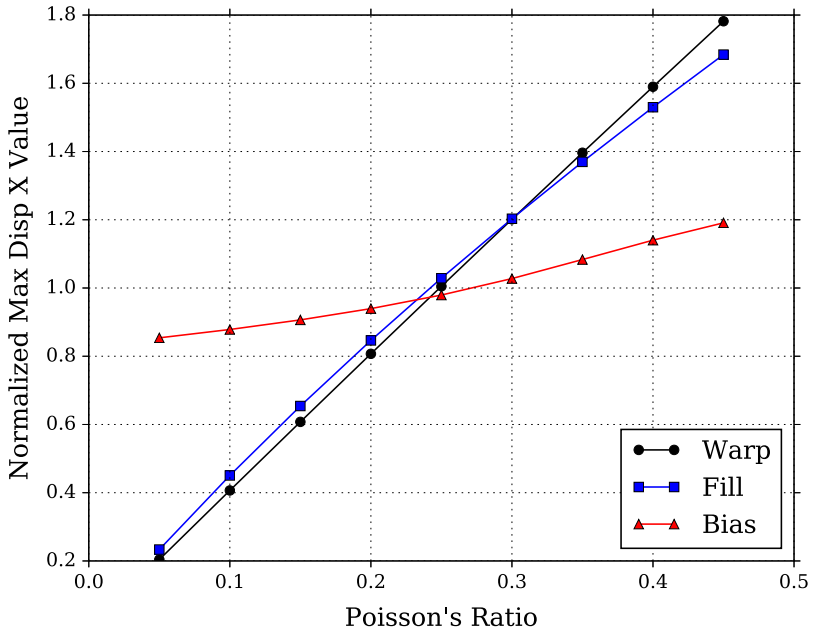

Fig. 6. The sensitivity to Poisson's ratio of the transverse displacement in the FE models of the warp, fill, and 45° bias uniaxial tests.

method. The data set contained each data point from the five uniaxial tests. It was useful to force the polynomial through the origin by removing the vertical intercept, because the FE model will only start from a zero stress–strain state. Different order polynomial fits were attempted. It was found that a fourth order polynomial had the lowest root mean square error for the warp uniaxial stress–strain behavior, while third order polynomials resulted in the lowest error values for the fill and 45° bias behavior. It is noted that the polynomials are excellent fits to the experimental stress–strain data. Both the coefficient of determination and the root mean square error of the fitted polynomials were used to quantify the quality of fits. The stress–strain polynomials are defined by Eqs. (1)–(3), where terms $\alpha_0 - \alpha_9$ represent the coefficients determined from the least squares fit.

$$\sigma_{warp}(\varepsilon_1) = \alpha_0\varepsilon_1 + \alpha_1\varepsilon_1^2 + \alpha_2\varepsilon_1^3 + \alpha_3\varepsilon_1^4 \tag{1}$$

$$\sigma_{fill}(\varepsilon_2) = \alpha_4\varepsilon_2 + \alpha_5\varepsilon_2^2 + \alpha_6\varepsilon_2^3 \tag{2}$$

$$\sigma_{45^\circ bias}(\gamma_{12}) = \alpha_7\gamma_{12} + \alpha_8\gamma_{12}^2 + \alpha_9\gamma_{12}^3 \tag{3}$$

Each of the fitted polynomials were differentiated to obtain the stiffness moduli as functions of strain for the non-linear orthotropic model. The stiffness moduli are defined by Eqs. (4)–(6), where terms $\beta_0 - \beta_9$ represent the variables of the non-linear orthotropic material model. The stiffness moduli polynomials were calculated from a strain of zero, to the maximum strain as experienced by the experimental tests in each material direction. The vales of the stiffness moduli were then inputed as a table into the NLELAST material model definition. The FE models are useful for providing some validation, and this is done by using the defined material model in the FE models to compare with the experimental test results.

$$E_1(\varepsilon_1) = \beta_0 + \beta_1\varepsilon_1 + \beta_2\varepsilon_1^2 + \beta_3\varepsilon_1^3 \tag{4}$$

$$E_2(\varepsilon_2) = \beta_4 + \beta_5\varepsilon_2 + \beta_6\varepsilon_2^2 \tag{5}$$

$$G_{12}(\gamma_{12}) = \beta_7 + \beta_8\gamma_{12} + \beta_9\gamma_{12}^2 \tag{6}$$

5. Characterization method 2: inverse analysis load–displacement

As an alternative method, an inverse analysis was performed to find a non-linear orthotropic material model that matches the virtual strain gauge load–displacement response. The material parameters (β terms of Eqs. (4)–(6)) are initially guessed. Then an optimization routine is used to minimize the difference between the load–displacement of the FE models and the experimental tests. The goal of the inverse analysis is to find the best material parameters, such that the FE model matches the experimental load–displacement response.

The load strain gauge displacement relationships can be seen in Figs. 7 and 8. The figures contain data points collected from all five uniaxial tests in a material direction. A polynomial, represented by the solid line, was fitted to the test data in each material direction. These polynomials were used in place of the experimental data to characterize the non-linear orthotropic material model. The experimental data from multiple runs were considered simultaneously, as the polynomials were fitted to the entire collection of data points. The polynomials were of excellent fit, as the lowest coefficient of determination of the polynomials was 0.959. Working with the polynomial is preferred over the data points, because the polynomial can be evaluated anywhere in the displacement range, so no interpolation would be needed between data points. The polynomials are used in place of the experimental data for the inverse analysis, for convenience and due to the high quality of fit.

Optimization is used to determine the best non-linear orthotropic material model by minimizing the difference between the physical uniaxial tests and the FE models. The uniaxial FE models are considered simultaneously to compute a single error value that describes the fit of the FE models to the virtual strain gauge test results. Design Optimization Tools (DOT) [16] wrapped in a Python script is used to run the FE models and determine the optimum material parameters.

Root mean square (RMS) error is used to determine the error between the FE model and the physical tests. The polynomials fitted to the load–displacement virtual strain gauge data from the physical uniaxial tests are represented by P_{warp}, P_{fill}, and P_{bias}. The

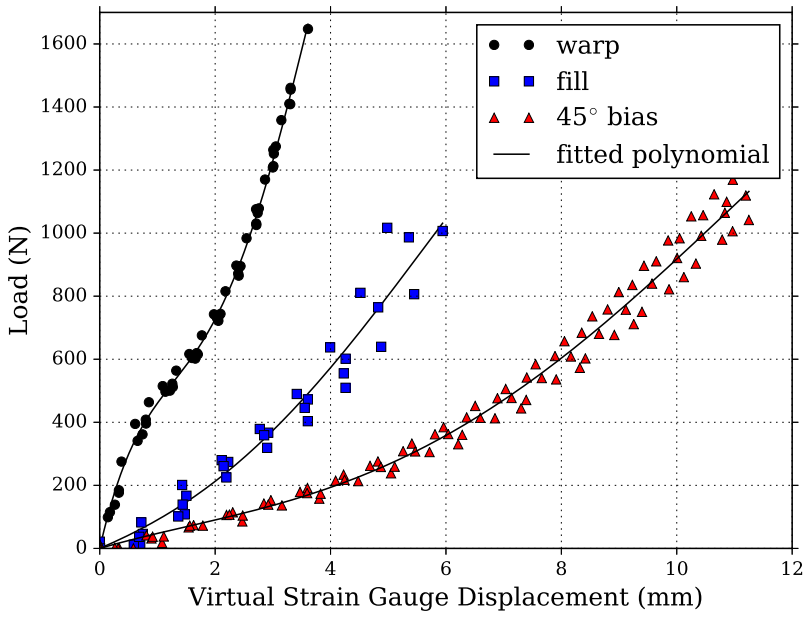

Fig. 7. Load strain gauge displacement values for the uniaxial tests in the warp, fill, and 45° bias material directions with fitted polynomial for the VALMEX® 7318.

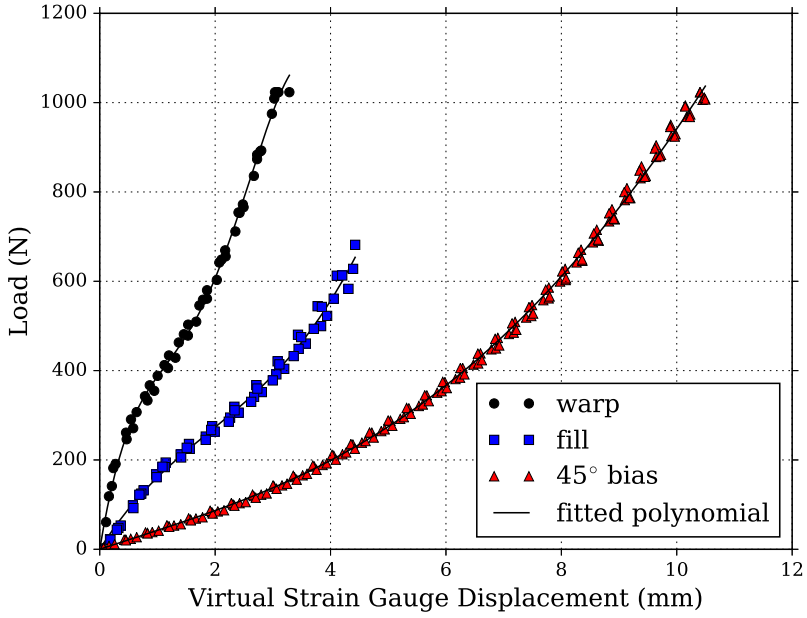

Fig. 8. Load strain gauge displacement values for the uniaxial tests in the warp, fill, and 45° bias material directions with fitted polynomial for the CF0700T.

FE models use 100 evenly spaced displacement increments when simulating a uniaxial test. Results of the FE model are only available at these specific increments. It is important that these increments are evenly distributed to avoid sampling errors, in which the error from a particular region of the test was sampled more often because more results where available in this area than other areas. A simple example of a non-linear FE model where this phenomenon would occur is any model that utilized adaptive time stepping. At each of the 100 load increments of the FE model, the load extracted from the FE model is represented by F_{warp}, F_{fill}, and F_{bias}. The load from the polynomials is compared directly with the load of the FE model at the 100 FE increments. Three RMS errors are calculated for each material direction, and can be seen in Eqs. (7)–(9).

$$e_{warp} = \sqrt{\frac{\sum_{i=1}^{100}(F_{warp}(i) - P_{warp}(i))^2}{100}} \tag{7}$$

$$e_{fill} = \sqrt{\frac{\sum_{i=1}^{100}(F_{fill}(i) - P_{fill}(i))^2}{100}} \tag{8}$$

$$e_{bias} = \sqrt{\frac{\sum_{i=1}^{100}(F_{bias}(i) - P_{bias}(i))^2}{100}} \tag{9}$$

The three RMS errors can be combined into a single error value $e_{uniaxial}$. It is possible to create the single error value by simply adding up the RMS of each material direction, though it was found that the optimizations were faster when considering the sum of the

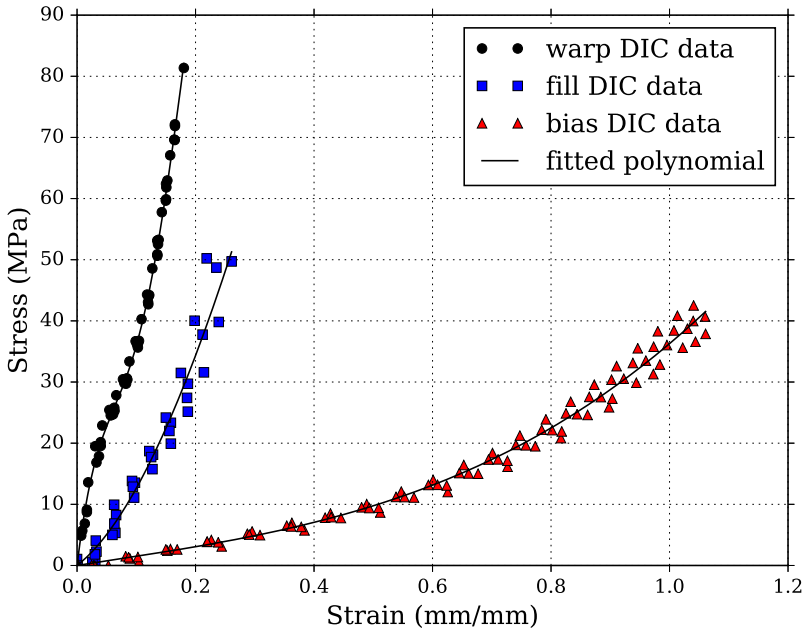

Fig. 9. The engineering stress and strain values with fitted polynomials for VALMEX® 7318.

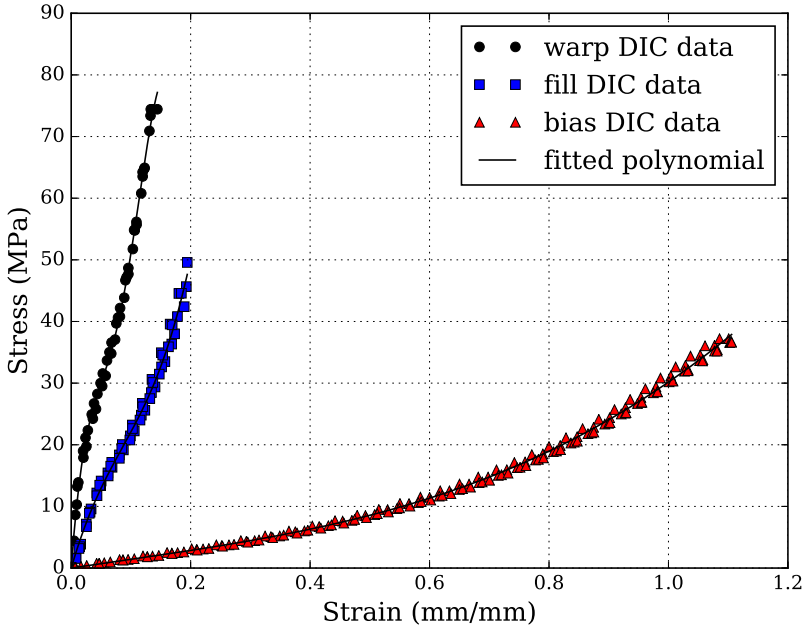

Fig. 10. The engineering stress and strain values with fitted polynomials for CF0700T.

square of RMS from each material direction as seen in Eq. (10). Each material direction is considered equally. It can be noted that weights can be added if matching the behavior of a particular uniaxial test direction was more important than the other directions. A $e_{uniaxial}$ value of 0.0 corresponds to a non-linear orthotropic material model in which the uniaxial FE models match the polynomials exactly. It is important to remember the fitted polynomials represent the experimental uniaxial load–displacement test data.

$$e_{uniaxial} = \sqrt{e_{warp}^2 + e_{fill}^2 + e_{bias}^2} \tag{10}$$

The overall objective function of the optimization can be expressed by minimizing the overall error of the FE models load–displacement results. The ideal material model will match the uniaxial virtual strain gauge load–displacement results exactly, while the best material model is defined mathematically as having the lowest objective function value. This optimization process is subject to two constraints, the first being that the moduli in the material model must remain positive for the entire strain range because a negative moduli for a positive strain is not sensible. The second being that all of the FE analyses are valid, in which case Marc outputs an exit code for each analysis of 3004. This is important as the optimization may attempt to try many material models that are numerically unstable, and results in FE models that can only be partially completed. Thus when an error code of 3004 is returned, it means that the FE model converged on all 100 load increments. The overall objective function can be seen in Eq. (11). The two constraints serve as logical flags for the constrained optimization.

Table 3
Optimization bounds used for the inverse analysis to determine the non-linear orthotropic material model.

Variable	Lower bound	Upper bound
β_0	0.25	2.0
β_1	−0.01	0.01
β_2	−0.001	0.001
β_3	−0.002	0.002
β_4	0.01	2.0
β_5	−0.01	0.01
β_6	−0.001	0.001
β_7	70.0	700.0
β_8	−50.0	50.0
β_9	−4.0	4.0

When a constraint is violated, a value of 1 is fed into the algorithm, while a value of −1 indicates a satisfied constraint. This type of true–false boolean constraint may be problematic for a gradient based optimization algorithm, however DOT deals with boolean constraints well by backtracking when encountering a violated constraint in the one dimensional search. It is important to mention that DOT's approach works well, provided that the optimization is started from a feasible point.

$$\begin{aligned} &\text{minimize}: && e_{uniaxial} \\ &\text{suchthat}: && E_1, E_2, G_{12} > 0 \quad \text{and} \\ & && \text{AllMarcExitCodes} = 3004 \end{aligned} \tag{11}$$

The β terms of Eqs. (4)–(6) are the variables the optimizer will use to determine the best non-linear orthotropic material model, however a reasonable starting point and the variable bounds are unknown. Suitable variable bounds were approximated to be one order of magnitude, larger and smaller, from the solution of the previous method. The bounds used for the optimization of both materials are provided in Table 3. An initial optimization was performed on β terms that began in the feasible region to satisfy the boolean constraints.

DOT parameters were used in their default configuration, including gradient step size, scaling, and convergence criteria. From the optimum of this initial optimization, a second optimization was run with a gradient step size one order of magnitude smaller than DOT's default. The second optimization typically resulted in the lowest obtained objective function for both materials. One can point out that a suitable starting point for the optimization would be the resulting material model variables from the stress–strain method, however this approach wasn't used because it was the intention to demonstrate that the inverse analysis could function independently of the stress–strain method. The Modified Method of Feasible Directions (MMFD) algorithm proved to be the most reliable gradient based optimization algorithm from the DOT library for the inverse problems considered here. It is wise to start the optimizations from multiple starting points to ensure

Table 4
Variables for the polynomials that define the non-linear orthotropic material models for the two types of PVC-coated polyester from the stress–strain and inverse load–displacement methods.

	VALMEX® 7318		CF0700T	
Variable	Method 1: direct	Method 2: inverse	Method 1: direct	Method 2: inverse
β_0	0.803338	0.808749	1.303904	1.007260
β_1	−0.00204	−0.00207	−0.00474	−0.00258
β_2	0.000218	0.000226	0.000679	0.000291
β_3	−0.00059	−0.00058	−0.00274	−0.00085
β_4	0.075277	0.076246	0.332784	0.346241
β_5	0.000107	0.000114	−0.00037	−0.00045
β_6	−8.2e-07	−7.5e-07	2.13e-05	3.09e-05
β_7	149.5966	270.589	145.1017	337.0310
β_8	−0.61890	−19.6316	−1.04362	−29.0470
β_9	0.073223	0.553649	0.062623	0.892731

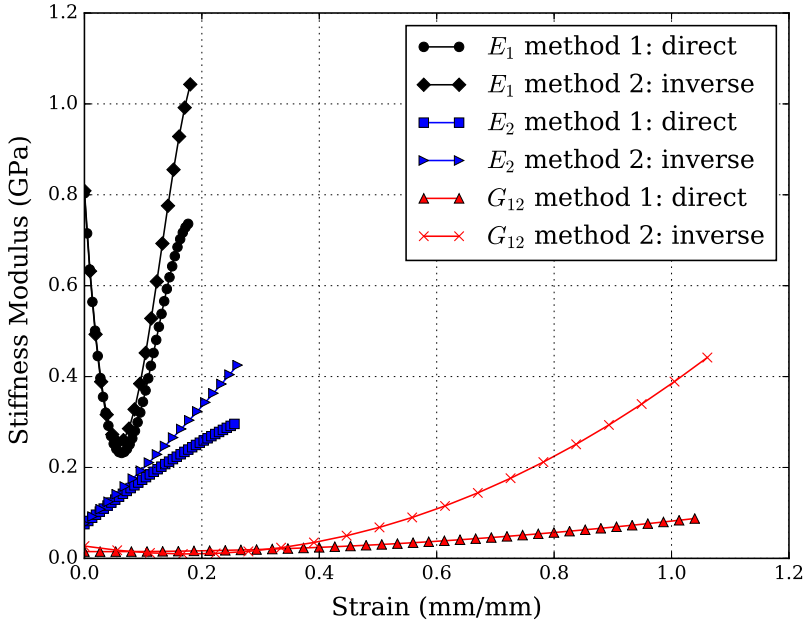

Fig. 11. Non-linear orthotropic material models for VALMEX® 7318 from the direct stress–strain and inverse load–displacement methods.

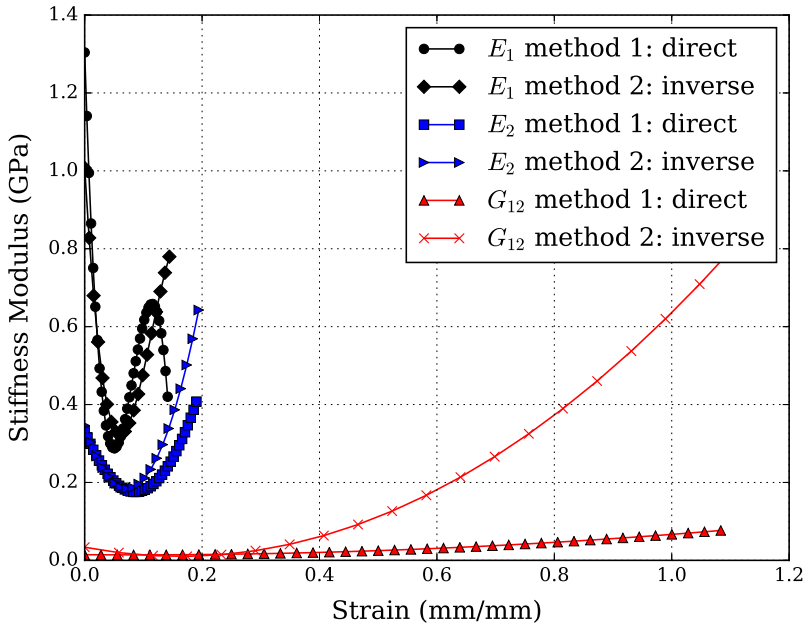

Fig. 12. Non-linear orthotropic material models for CF0700T from the direct stress–strain and inverse load–displacement methods.

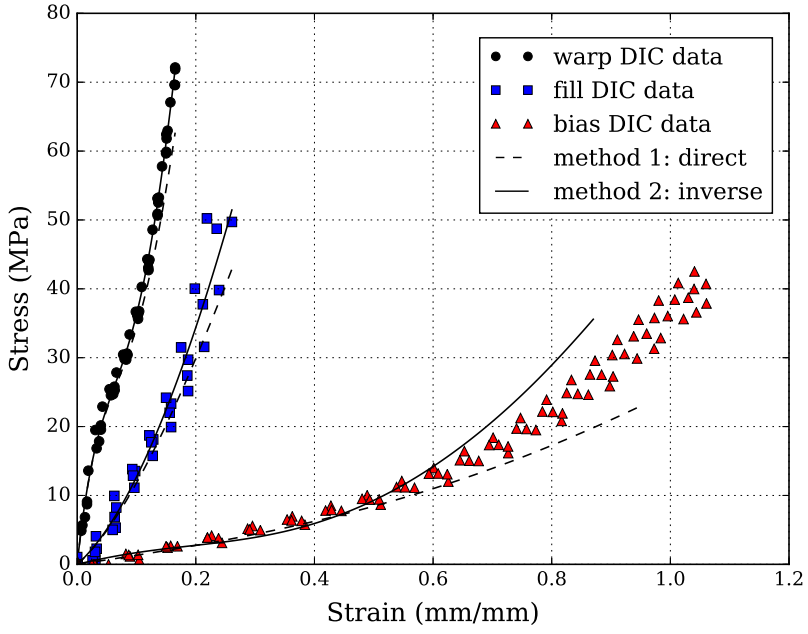

Fig. 13. Stress–strain results of the FE models with the two different material models compared to the experimental uniaxial data for VALMEX® 7318.

the best material model is found, and to avoid selecting a local minimum in the design space as the best material model.

6. Results

Two different methods were used to determine non-linear orthotropic material models for VALMEX® 7318 and CF0700T. The β terms that define the material models are provided, and the material models are compared directly. It is expected that the material models will produce stress–strain and load–displacement relationships that differ from the experimental uniaxial tests, because of issues with the continuum assumption at the large strains experienced. To demonstrate these differences, the results of the FE uniaxial models with material models from both methods are compared directly to the experimental test data.

The β terms that define the non-linear orthotropic material models are presented in Table 4. Subtle differences in the values can be noted for the two different methods for a particular material. The non-linear orthotropic material models are plotted together in Figs. 11 and 12. The stress–strain method produced a material model that is similar to the inverse load–displacement method. In addition, the stiffness moduli of the different materials appears to be similar.

The non-linear orthotropic material models were used in FE models replicating the experimental uniaxial test. It is important to understand the ability of the FE models to replicate the behavior

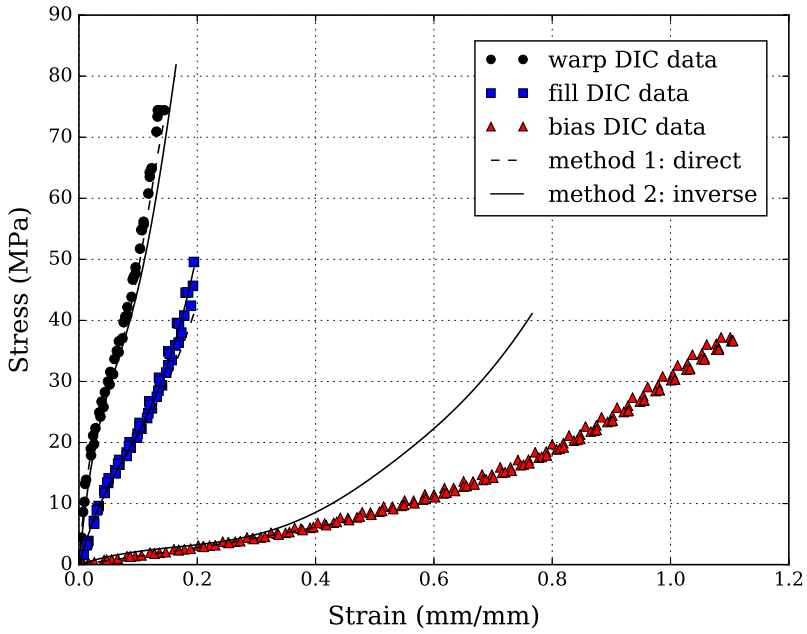

Fig. 14. Stress–strain results of the FE models with the two different material models compared to the experimental uniaxial data for CF0700T.

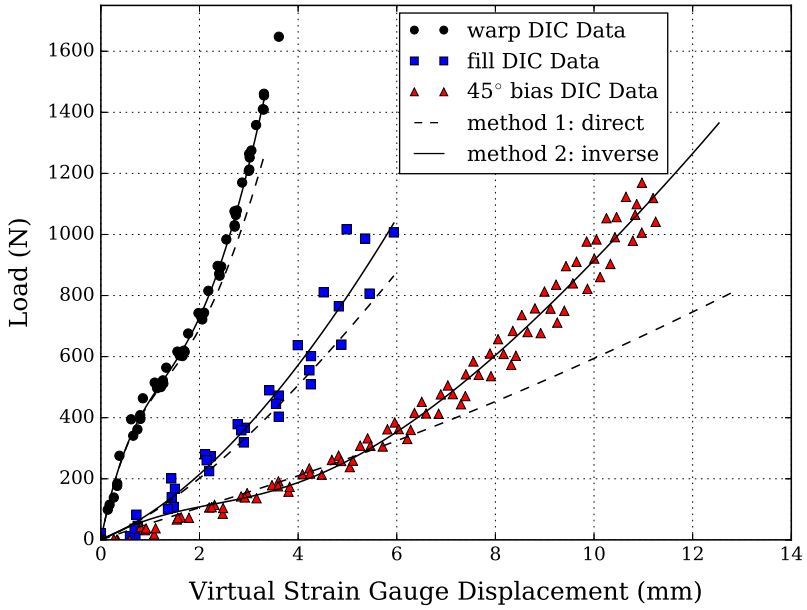

Fig. 15. Virtual strain gauge results of the FE models with the two different material models compared to the experimental uniaxial data for VALMEX® 7318.

of the physical tests, before considering the material model in the modeling of a structure. Thus the results of the FE models were compared directly to the uniaxial test data.

The experimental stress–strain values are compared to FE results in Figs. 13 and 14. For both materials, in the warp and fill directions, the non-linear orthotropic material models do an excellent job at replicating the stress–strain behavior of the materials. Either the direct stress–strain method or inverse load–displacement method produces a stress–strain curve that is analogous to the experimental data in the warp and fill uniaxial test directions. Unfortunately the same cannot be stated for the 45° bias uniaxial test. Both methods fail to capture the behavior of the 45° bias test at high strains. For the CF0700T PVC-coated polyester, the 45° bias FE model was unstable and failed to converge to the maximum strain.[1] This is why in Fig. 14, the stress–strain curve resulting from the bias FE model terminates before 0.2 strain instead of the maximum 0.5 strain. The inverse load–displacement non-linear orthotro-

[1] From the author's experience, the only way to get the 45° bias model to converge with this particular set of material model parameters is to use a coarser mesh. The convergence problem is linked to an element becoming singular during the deformation. Generally when a finer mesh is used, the number of singular elements increases. The results of the model with a coarser mesh were not shown in this result section, because it would not be a fair comparison with the other FE models.

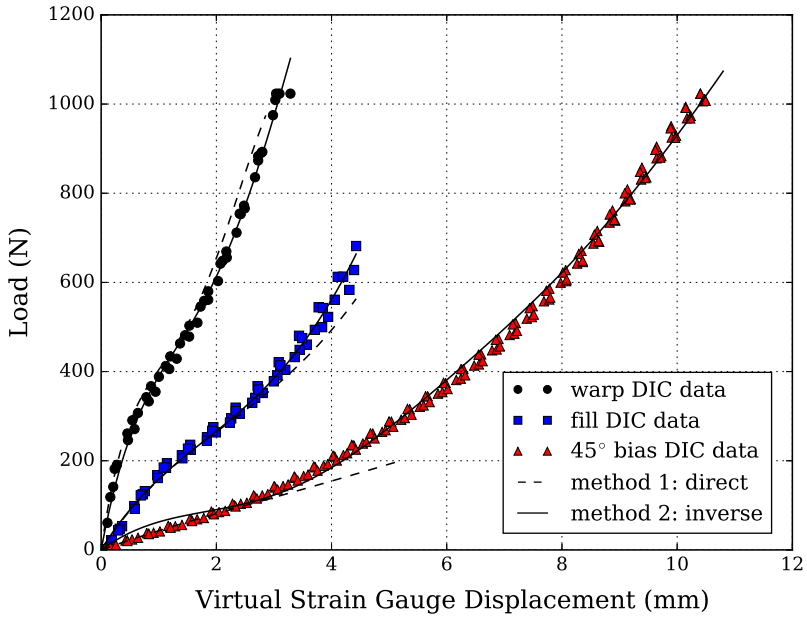

Fig. 16. Virtual strain gauge results of the FE models with the two different material models compared to the experimental uniaxial data for CF0700T.

Table 5
Coefficient of determination for each stress–strain or load–displacement material comparison from the FE results using the non-linear orthotropic material models.

	VALMEX® 7318		CF0700T	
Material comparison	Method 1: direct	Method 2: inverse	Method 1: direct	Method 2: inverse
R^2 of warp stress–strain	0.97	0.99	0.99	0.94
R^2 of warp load–displacement	0.96	0.99	0.98	0.99
R^2 of fill stress–strain	0.92	0.95	0.97	0.99
R^2 of fill load–displacement	0.92	0.95	0.97	0.99
R^2 of 45° bias stress–strain	0.84	0.82	N/A	0.0
R^2 of 45° bias load–displacement	0.71	0.98	N/A	0.99
Average R^2 for method	0.89	0.95	N/A	0.82

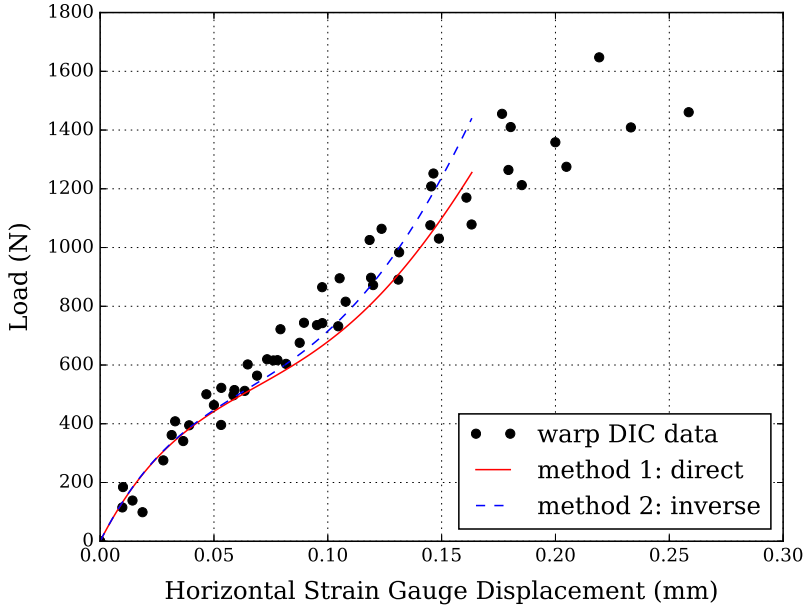

Fig. 17. Transverse displacement of the FE models compared with the experimental warp uniaxial test data for VALMEX® 7318.

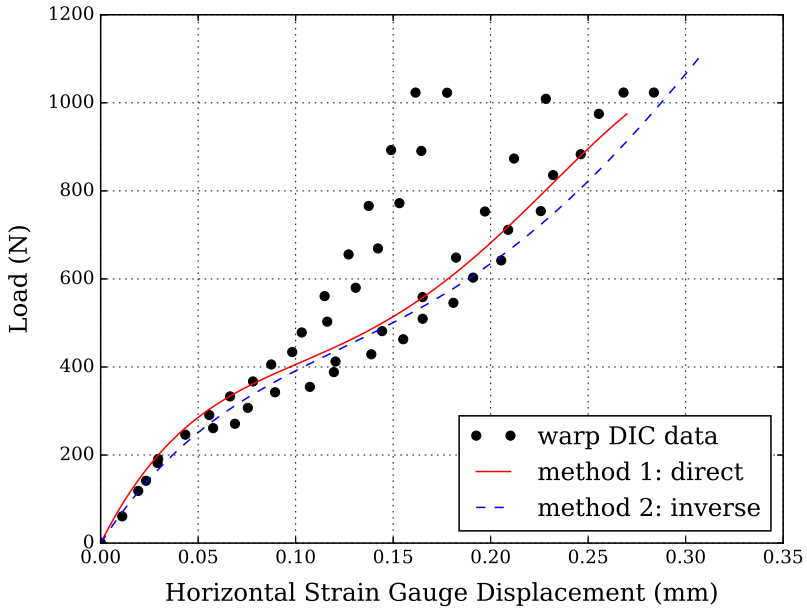

Fig. 18. Transverse displacement of the FE models compared with the experimental warp uniaxial test data for CF0700T.

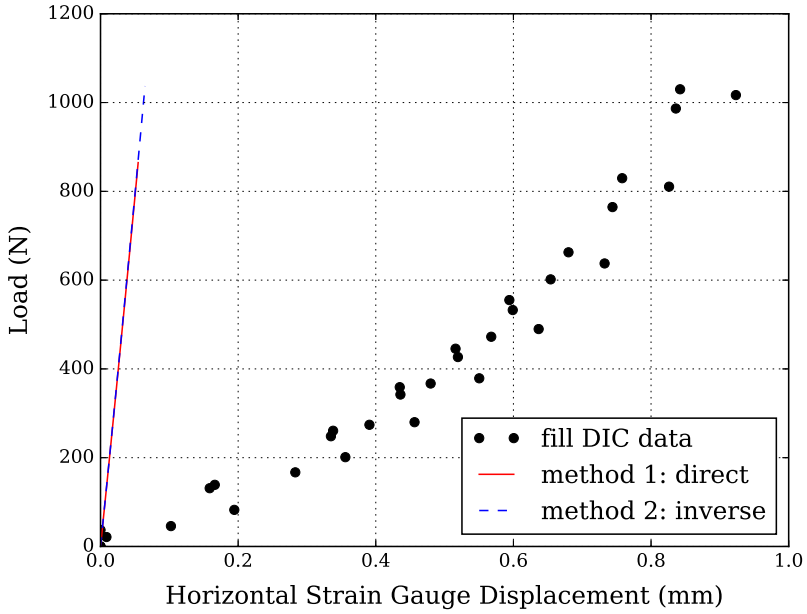

Fig. 19. Transverse displacement of the FE models compared with the experimental fill uniaxial test data for VALMEX® 7318.

pic material model also severely over predicts the response of the bias extension test, though it appears the inverse load–displacement method produces a material model that better represents the 45° bias uniaxial test behavior.

The axial virtual strain gauge displacements are compared to the results of the FE models in Figs. 15 and 16. Again in the material warp and fill directions, it can be noted that both the direct stress–strain and inverse load–displacement methods produce non-linear orthotropic models that match the physical uniaxial behavior. The inverse load–displacement method was defined to match the load–displacement behavior, and effectively accomplishes this by matching the load–displacement behavior of the experimental tests data for each material direction almost exactly. The direct stress–strain method produces a non-linear orthotropic material model that severely under predicts the load–displacement response of the 45° bias test.

The coefficient of determination was calculated for each comparison of the non-linear orthotropic FE models to the experimental uniaxial data. As seen in Table 5, the inverse load–displacement method produced similar coefficient of determinations. This suggests that the inverse load–displacement method produced non-linear orthotropic material models that are analogous to the direct stress–strain method. N/A in the table represents the FE models that were unstable, and failed to converge.

An excellent material model would be able to accurately predict both the axial and transverse load–displacement material response. The transverse displacement of the FE models were compared to the results from a virtual horizontal strain gauge on the experimental uniaxial tests. It is seen that the non-linear orthotropic material model matches the transverse load–displacement response of the materials in the warp direction, as seen in Figs. 17 and 18. This suggests that the use and determination of the Pois-

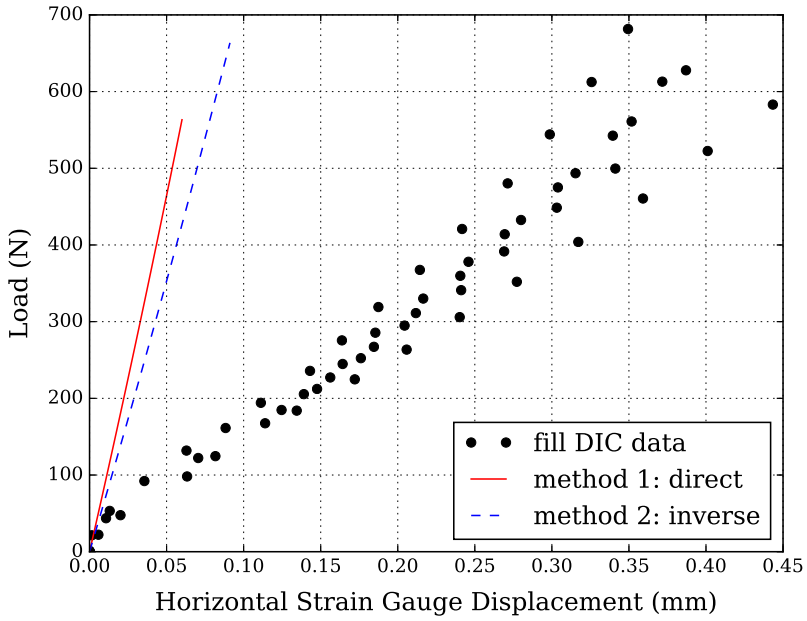

Fig. 20. Transverse displacement of the FE models compared with the experimental fill uniaxial test data for CF0700T.

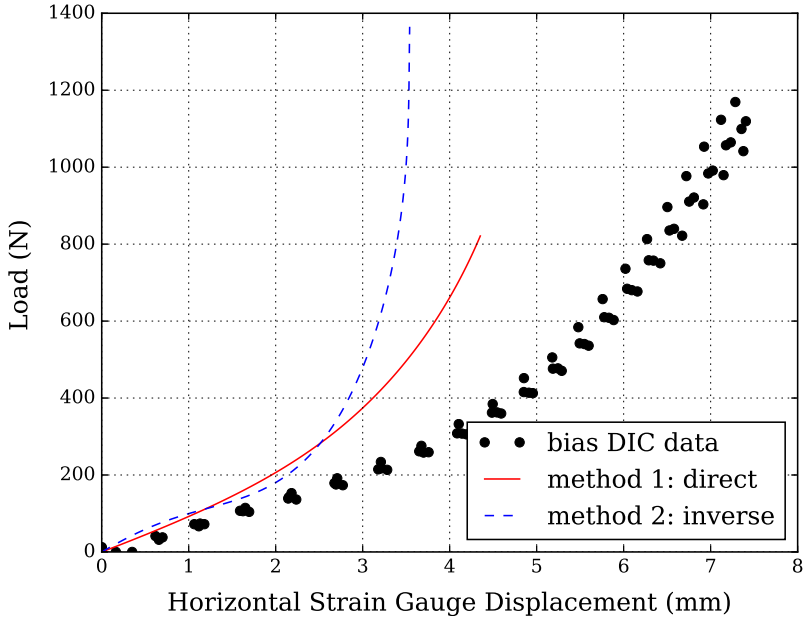

Fig. 21. Transverse displacement of the FE models compared with the experimental 45° bias uniaxial test data for VALMEX® 7318.

son's ratio (ν_{12}) adequately matches the response of both materials in the warp direction. The transverse load–displacements, seen in Figs. 19 and 20, are poor and over estimated for the fill uniaxial test. Potentially this shows that the non-linear orthotropic material model behaves fundamentally different than the physical behavior of the PVC-coated polyester. It is interesting to point out that the transverse comparison in the 45° bias direction yields a different result, as seen in Figs. 21 and 22. It appears that the direct stress–strain method doesn't match the transverse behavior of the 45° bias extension test, while the material model from the inverse load–displacement analysis matches the transverse displacement extremely well at low strains. Though the good fit quickly deteriorates at higher strains, potentially demonstrating the limitations of the non-linear orthotropic material model.

7. Conclusion

Non-linear orthotropic material models were determined for two different PVC-coated polyesters. The material models were determined using two different methods. The first method determined the non-linear orthotropic model by differentiating the stress–strain response from uniaxial tests. The second method utilized an inverse analysis that produced a non-linear orthotropic material model through numerical optimization, by matching the FE models to the uniaxial load–displacement response. The two approaches produce different material model parameters, however at small strains the material behavior from the different methods is comparable. Due to breakdowns in the plane-stress continuum assumption and the large strains exposed in the uniaxial models, it is impossible to match the complete stress–strain and load–dis-

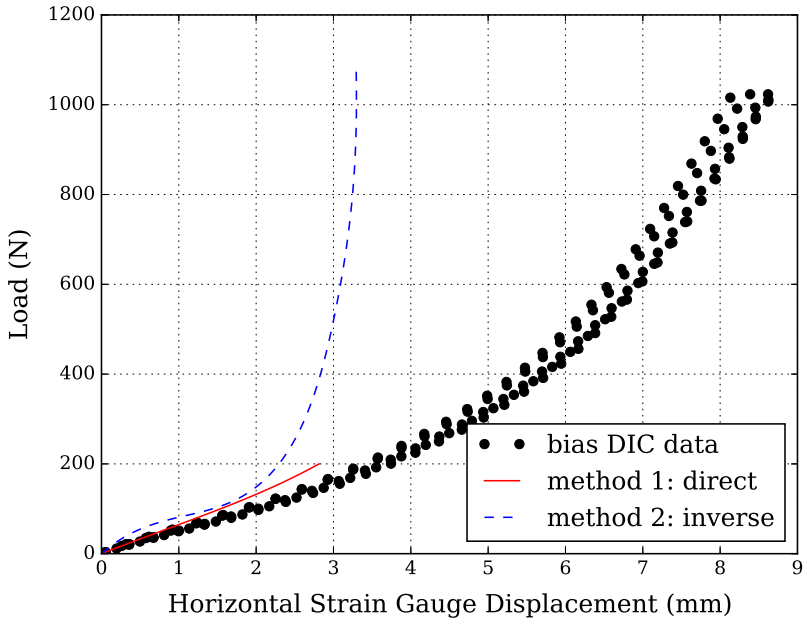

Fig. 22. Transverse displacement of the FE models compared with the experimental 45° bias uniaxial test data for CF0700T.

placement material responses at high strains with this material model.

The derived non-linear orthotropic models failed to capture the complete uniaxial response in the 45° bias extension test for both PVC-coated polyesters. The direct stress–strain method produced a non-linear orthotropic material model that matched the experimental stress–strain response better than the material model from the inverse load–displacement method. While the inverse analysis proved useful, as a method to accurately reproduce the load–displacement behavior of the experimental bias test seen in Figs. 15 and 16. Though due to the limitations of the non-linear orthotropic model, the inverse method produced a model that over predicted the stress–strain response of the bias extension test. There is an effective trade-off between matching either the stress–strain or the load–displacement response with the 45° bias extension test at high strains, because the 45° bias test produces a complex load case that the hypoelastic non-linear orthotropic material model is incapable of recreating.

The Poisson's ratio (ν_{12}) was determined using the transverse and axial displacements from the warp uniaxial tests. It was demonstrated that by simply taking the average of calculated Poisson's ratios, a suitable Poisson's ratio can be determined for the warp uniaxial test. This was demonstrated for the material model by the traverse load–displacement results of a warp uniaxial test, as seen in Figs. 17 and 18. For the warp uniaxial test, all non-linear orthotropic material models matched the axial and transverse displacements excellently. However the Poisson's effect observed in the experimental fill and bias uniaxial tests is vastly different from what the non-linear orthotropic material model is capable of offering. With the combination of transverse displacement results for the fill direction in Figs. 19 and 20 and the transverse displacement sensitivity study of Fig. 6, it was concluded that it was not possible for the presented non-linear orthotropic material model to simultaneously match the transverse displacements in both the warp and fill uniaxial tests.

Acknowledgments

This research did not receive any specific grant from funding agencies in the public, commercial, or not-for-profit sectors.

References

[1] Cavallaro PV, Sadegh AM, Quigley CJ. Decrimping behavior of uncoated plain-woven fabrics subjected to combined biaxial tension and shear stresses. Text Res J, 0040-5175 2007;77(6):403–16. http://dx.doi.org/10.1177/0040517507080258.
[2] Luchsinger RH, Sydow A, Crettol R. Structural behavior of asymmetric spindle-shaped Tensairity girders under bending loads. Thin-Walled Struct 2011;49(9):045–1053. http://dx.doi.org/10.1016/j.tws.2011.03.012.
[3] Nguyen T-T, Ronel S, Massenzio M, Apedo KL, Jacquelin E. Analytical buckling analysis of an inflatable beam made of orthotropic technical textiles. Thin-Walled Struct, 0263-8231 2012;51(0):186–200. http://dx.doi.org/10.1016/j.tws.2011.10.017.
[4] Galliot C, Luchsinger RH. Structural behavior of symmetric spindle-shaped Tensairity girders with reinforced chord coupling. Eng Struct 2013;56:407–16. http://dx.doi.org/10.1016/j.engstruct.2013.05.023.
[5] Cavallaro PV, Johnson ME, Sadegh AM. Mechanics of plain-woven fabrics for inflated structures. Compos Struct 2003;61(4):375–93. http://dx.doi.org/10.1016/S0263-8223(03)00054-0.
[6] Gosling, Bridgens, Testing Material. Computational mechanics – a new philosophy for architectural fabrics. Int J Space Struct, 0266-3511 2008;23(4):215–32. http://dx.doi.org/10.1260/026635108786959870.
[7] Chen S, Ding X, Yi H. On the anisotropic tensile behaviors of flexible polyvinyl chloride-coated fabrics. Textile Res J, 0040-5175 2007;77(6):369–74. http://dx.doi.org/10.1177/0040517507078791.
[8] Klosowski P, Komar W, Woźnica K. Finite element description of nonlinear viscoelastic behaviour of technical fabric. Constr Build Mater, 09500618 2009;23(2):1133–40. http://dx.doi.org/10.1016/j.conbuildmat.2008.06.002.
[9] Galliot C, Luchsinger R. A simple model describing the non-linear biaxial tensile behaviour of PVC-coated polyester fabrics for use in finite element analysis. Compos Struct, 02638223 2009;90(4):438–47. http://dx.doi.org/10.1016/j.compstruct.2009.04.016.
[10] Ambroziak A, Kłosowski P. Mechanical properties for preliminary design of structures, made from PVC coated fabric. Constr Build Mater, 09500618 2014;50:74–81. http://dx.doi.org/10.1016/j.conbuildmat.2013.08.060.
[11] MSC Marc, Volume A: Theory and User Information, MSC Software Corporation; 2014.
[12] Garbowski T, Maier G, Novati G. On calibration of orthotropic elastic-plastic constitutive models for paper foils by biaxial tests and inverse analyses. Struct Multi Optim, 1615-147X 2011;46(1):111–28. http://dx.doi.org/10.1007/s00158-011-0747-3.
[13] ASTM D751 – 06, Standard Test Methods for Coated Fabrics, January; 2011.
[14] LaVision GmbH, Product-Manual DaVis 8.2 Software, Göttingen, Germany, 8.2, edn.; 2014.
[15] LaVision GmbH, Product-Manual StrainMaster Portable, Göttingen, Germany, 8.2, edn.; 2014
[16] Vanderplaats Research &, Development Inc., DOT Users manual, Colorado Springs, CO, 5.x, edn.; 2001.